ELSEVIER

International Journal of Mass Spectrometry 193 (1999) 87–99

International Journal of Mass Spectrometry

Correction of instrumentally produced mass fractionation during isotopic analysis of Fe by thermal ionization mass spectrometry

Clark M. Johnson*, Brian L. Beard

Department of Geology and Geophysics, University of Wisconsin, Madison, WI 53706, USA

Received 22 February 1999; accepted 29 July 1999

Abstract

High-precision (~0.015%/mass) isotope ratio measurements of Fe may be obtained by using magnetic-sector thermal ionization mass spectrometry (TIMS), where rigorous correction of instrumentally produced mass fractionation can be made. Such corrections are best done by using a double-spike approach, which was first introduced several decades ago. However, previous derivations do not lend themselves to the high-precision isotope analysis that modern TIMS instruments are capable of because of various assumptions of mass fractionation laws or constant atomic weights. Moreover, some of these previous approaches took iterative approaches to the calculation, and none presented detailed error propagations. Here we present a completely general derivation to the double-spike approach that may be used for any appropriate isotope system and is applicable to the mass fractionation laws that are known to occur in TIMS. In addition, we present an assessment of error propagation as a function of algorithm and spike isotope composition. This approach has produced the highest precision Fe isotope ratio measurements yet reported, on the order of ±0.2 to 0.3 per mil for the $^{54}Fe/^{56}Fe$ ratio, that correct for instrumentally produced mass fractionation and yet retain natural, mass-dependent isotopic variations in samples. (Int J Mass Spectrom 193 (1999) 87–99) © 1999 Elsevier Science B.V.

Keywords: Fe; Isotope; Mass spectrometry; Thermal ionization; Double spike

1. Introduction

There have been relatively few isotopic studies of intermediate-mass elements, in comparison to studies of mass-dependent fractionation of the light stable isotopes (e.g. [1]), or studies of heavier elements that are part of radioactive decay systems (e.g. [2]). However, intermediate-mass elements may undergo natural, mass-dependent isotopic fractionation, as has been discussed for Ca [3–5]. In the case of Fe, its importance in metabolism, as well as nucleosynthetic processes, has inspired a number of previous Fe isotope investigations (Table 1; [6–12]). Most of these studies used magnetic-sector TIMS in an effort to maximize the precision. Alternative methods, such as inductively coupled plasma mass spectrometry (ICP-MS) have advantages in higher ionization efficiencies as compared to TIMS, but suffer from ArN^+ and ArO^+ interferences on ^{54}Fe and ^{56}Fe, respectively, which presents significant difficulty in obtaining precise isotope ratios for all of the Fe isotopes.

A significant limitation of isotopic analysis using TIMS is the potentially large and variable mass fractionation that occurs in a TIMS source. A common approach to removing instrumentally produced

* Corresponding author. E-mail: clarkj@geology.wisc.edu

PII S1387-3806(99)00158-X

Table 1
Summary of various studies of iron isotope measurements of normal Fe by different analytical techniques[a]

Method	$^{54}Fe/^{56}Fe$	$^{57}Fe/^{56}Fe$	$^{58}Fe/^{56}Fe$	Remarks	Ref.
TIMS quadrupol mass spectrometry	0.0618 ± 3.2‰	0.0243 ± 12.3‰	0.003 61 ± 52.6‰	Rapid analysis method well suited for Fe nutritional tracer studies where the variation in Fe isotope ratios are set to vary over a wide range.	[6]
SIMS (Internal normalization)	≡0.066 57	0.022 58 ± 0.74‰	0.002 927 ± 2.71‰	Data are internally normalized to $^{54}Fe/^{56}Fe$. Instrumental mass bias is strongly dependent on the Fe content of the analyzed phase. Ni isobar corrections can be extreme. Internal normalization is not suitable for evaluating mass-dependent fractionation. In situ spot analyses are possible.	[7]
TIMS (Internal normalization)	≡0.062 669	0.023 261 ± 0.10‰	0.003 113 2 ± 1.39‰	Data were internally normalized to $^{54}Fe/^{56}Fe$. Internal normalization is not suitable for evaluating mass-dependent fractionation, but is an excellent method for evaluation of nucleosynthesis processes.	[8]
TIMS external normalization to Fe standards by ion counting	0.063 371 ± 0.6‰	0.023 149 ± 0.3‰	0.003 081 6 ± 4.0‰	Instrumental mass bias determined by analysis of Fe isotope reference materials and assumes samples and standards fractionate identically. This requires highly controlled analysis conditions; 0.1–1 μg Fe used for an analysis measured on ion-counting Daly multiplier.	[9,10]
TIMS external normalization to Fe standards measured on Faraday detectors	0.063 70 ± 2.1‰	0.023 096 ± 1.6‰	0.003 071 0 ± 4.1‰	Instrumental mass bias for $^{54}Fe/^{56}Fe$ empirically measured using Fe isotope reference materials, other Fe isotope ratios internally normalized to $^{54}Fe/^{56}Fe$. Assumes samples and standards fractionate identically requiring highly controlled analysis conditions; 10 μg Fe used for an analysis measured on Faraday detectors.	[11]
Negative TIMS	0.063 623 ± 0.7‰	0.023 106 ± 0.3‰	0.003 079 9 ± 0.6‰	Instrumental mass bias is limited by analyzing a high-molecular-weight polyatomic species FeF_4^-; 6 μg of Fe used for an analysis.	[12]
TIMS double spike method	0.063 679 ± 0.30‰	0.023 088 ± 0.15‰	0.003 061 6 ± 0.28‰	Corrections for instrumental mass bias are rigorously made using a mixed ^{54}Fe–^{58}Fe double spike. Analysis method is ideally suited for evaluating both nucleosynthesis and mass-dependent isotope fractionation processes; 4 μg of Fe used for an analysis, measured on Faraday detectors.	This study

[a] All errors are quoted in relative per mil at the one standard deviation level. The error for the TIMS quadrapole data [6] is based on 7 analyses of an Fe standard. The error for the SIMS data [7] is calculated from the reported values of 4 mineral and metal standards. The errors for the TIMS data from [8] is calculated from the reported values of 5 normal Fe solutions. The error for the TIMS data from [9–11] is calculated from the reported precision of Fe standard material; errors for samples reported in [9,10] are estimated to be approximately an order of magnitude higher, based on inconsistent variations between Fe isotope ratios. The errors for the negative TIMS data [12] are calculated from 6 analyses of an Fe standard. The errors for TIMS double-spike data (this study) are based on 21 analyses of an ultrapure Fe standard (Table 4), and reflect relative errors; absolute uncertainties are larger due to uncertainty in spike isotope composition (see text).

mass fractionation is to adjust the measured ratios of interest to a single reference ratio. This approach, often referred to as "internal normalization," is useful where one isotope may independently vary due to radiogenic in-growth from a radioactive parent isotope (e.g. [2]), or from nucleosynthetic processes (e.g.

[2,8]). Although internal normalization is capable of producing high-precision Fe isotope ratios, on the order of ±0.01% (or 0.1 per mil) by using TIMS [8], this approach completely removes any natural, mass-dependent isotopic fractionation that may exist in the sample.

Two approaches may be taken that correct for instrumentally produced mass fractionation and yet retain natural, mass-dependent isotopic variations in samples. One is an empirical approach, where the average instrumental mass fractionation is estimated by isotopic analysis of gravimetrically prepared isotopic standards. This approach was applied to Fe by Taylor et al. [13] and Dixon et al. [9,10], who report the reproducibility of Fe standards as ±0.3 per mil (‰) per mass. However, the data reported for samples [9] are considerably more variable and contain internal inconsistencies among the Fe isotope ratios, suggesting that the true precision on samples of unknown isotopic composition and matrices is on the order of 1–3 per mil per mass using the empirical approach.

It has long been known that the most rigorous approach for correcting instrumentally produced mass fractionation and, at the same time, retaining natural isotope variations in samples, is the double-spike method (e.g. [13–15]). The advantage of the double-spike approach is that it is not affected by variations in sample matrix, sample loading, or source conditions, factors that can produce significant uncertainties in the empirical approach to correcting instrumental mass fractionation.

In this contribution, we present a completely general formulation of the double-spike approach that avoids previous approximations and assumptions that either prevented precise isotopic measurements, involved iterative calculations, or were derived for a specific isotope system.

2. Double-spike method

The double-spike technique is superior to the approaches that have been previously taken for Fe isotope analysis, because it allows rigorous instrumental mass fractionation corrections to be made, and simultaneously preserving naturally occurring, mass-dependent isotope variations (e.g. [13–15]). The double-spike approach can only be used for elements with four or more isotopes and in its most general application, requires two analyses; an analysis of an unspiked aliquot of the unknown (sample), and an analysis of a mixture that is composed of the sample and a tracer (spike) of known isotopic composition, where the spike is composed of two of the isotopes of the element of interest. Iron has four naturally occurring isotopes and high-purity enriched tracers of all four iron isotopes are available.

The double-spike method has been extensively discussed in the literature, initially in regard to correcting instrumental mass fractionation during Pb isotope analysis (e.g. [3,14–21]), prior to establishment of the silica-gel method for minimizing isotopic fractionation for Pb analysis using TIMS (e.g. [22]). There has been recent renewed interest in the double-spike approach in studies of natural, mass-dependent isotopic fractionation of Ca and Fe [3–5,23–25]. However, previous discussions on the double-spike method have shortcomings in their application to the general problems involved in modern, high-precision isotopic measurements of naturally fractionated samples because they either (1) followed an iterative approach [13,14], (2) made simplifying assumptions in terms of constant atomic weights of spike and sample [17,18], or (3) assumed very simple linear mass fractionation laws [14,19,20] that are not applicable to isotopic analysis of elements that follow more complex instrument-produced mass fractionation, such as an exponential form (e.g. [3,26]); these shortcomings produce very large errors at the per mil level of precision, which are too large to be useful for intermediate-mass elements. As will be discussed in Sec. 2.1, several of these previous studies use more complex (although still “linear”) mass fractionation laws [15,16,21] that may be adapted to approximate exponential mass fractionation [3]. However, none of the above studies provide completely general solutions to the double-spike approach. Here we present a completely general derivation to the double-spike method that is explicitly related to the three-dimensional geometry of the approach, and which closely

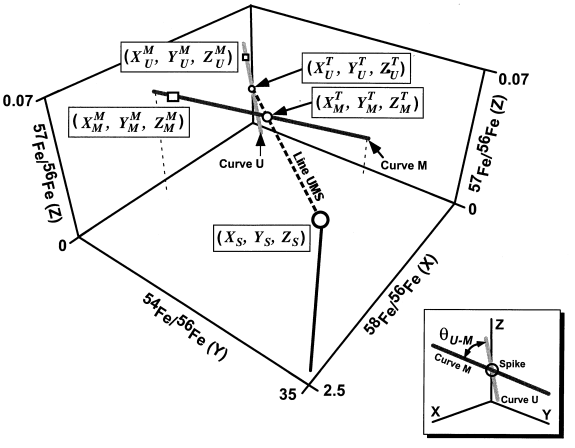

Fig. 1. Three-dimensional illustration of unknown (sample)–mixture–spike relations for Fe isotopes, following the approach outlined by Hofmann [19]. True dimensions are illustrated using normal Fe and the U.W. Madison ^{58}Fe–^{54}Fe double spike. The specific case where $m_j = 56$ is shown here. Circles represent true isotope compositions for the unknown (X_U^T, Y_U^T, Z_U^T), spike + sample mixture (X_M^T, Y_M^T, Z_M^T), and spike (X_S, Y_S, Z_S). Curves *U* and *M* are mass fractionation curves (shown as true linear fractionation for simplicity) for unknown (sample) and mixture (spike + sample), respectively. Curve *U* calculated using $f = -0.5$ to $+0.5$. Curve *M* calculated using $f = -0.4$ to $+0.4$. Arbitrary measured (fractionated) compositions are shown as squares for the unknown (X_U^M, Y_U^M, Z_U^M) and mixture (X_M^M, Y_M^M, Z_M^M). Line *UMS* connects the true isotopic compositions of the unknown, mixture, and spike. Inset shows the three-dimensional view (true relative scale) down line *UMS*, which illustrates the angle θ_{U-M}, which is defined as the angle between the unknown and mixture fractionation lines. Maximization of θ_{U-M} tends to minimize propagated errors in the double-spike method.

approximates exponential mass fractionation. We also discuss in detail propagated errors as a function of the spike composition, spike to sample ratios, and uncertainties in the measured isotope ratios.

2.1. Geometrical presentation

Hofmann [19] provided an excellent three-dimensional visualization of the double-spike approach, which is presented in the notation used here in Fig. 1. Isotope ratios *X*, *Y*, and *Z* are generally defined as m_i/m_j, where m_i is variable and m_j is a constant for a given set of isotope ratios (such as $X = {}^{58}Fe/{}^{56}Fe$, $Y = {}^{54}Fe/{}^{56}Fe$, and $Z = {}^{57}Fe/{}^{56}Fe$ in Fig. 1). The geometry of the double-spike method requires a common denominator isotope (m_j) so that mixing curves are straight lines. The true isotopic compositions of the unknown (X_U^T, Y_U^T, and Z_U^T), sample + spike mixture (X_M^T, Y_M^T, and Z_M^T), and spike (X_S, Y_S, and Z_S) must lie along a mixing line *UMS* (Fig. 1). However, in general, the measured isotopic compositions for the unknown (X_U^M, Y_U^M, and Z_U^M) and mixture (X_M^M, Y_M^M, and Z_M^M) will lie along mass fractionation curves that pass through the true isotopic ratios; these curves are illustrated as straight lines in Fig. 1 for simplicity, but they may follow any mass fractionation law. The precision that the line *UMS* is determined directly relates to the precision of the calculation of the true isotopic composition of the unknown (X_U^T, Y_U^T, and Z_U^T). The uncertainty in the line *UMS* is in part a function of the angle between the unknown and mixture mass fractionation curves (curves *U* and *M* in Fig. 1, respectively); this angle is defined as θ_{U-M}, and is discussed below in Sec. 3 on error propagation. The spike isotopic composition (X_S, Y_S, and Z_S) shown in Fig. 1 is that of our U.W. Madison ^{58}Fe–^{54}Fe spike.

2.2. Mass fractionation laws

A number of mass fractionation "laws" have been used in TIMS analysis. The simplest is often described as "linear mass fractionation," which Hart and Zindler [27] define as

$$\frac{Y_U^M - Y_U^T}{Y_U^T} = \frac{a_Y}{a_X}\frac{X_U^M - X_U^T}{X_U^T} = \frac{a_Y}{a_Z}\frac{Z_U^M - Z_U^T}{Z_U^T} \quad (1)$$

Isotope ratios are previously defined and a_X, a_Y, and a_Z are mass-difference coefficients, defined as

$$a_X = m_{i-j}^X, \qquad a_Y = m_{i-j}^Y, \qquad a_Z = m_{i-j}^Z \quad (2)$$

where $m_{i-j} = (m_i - m_j)$, and is defined as the mass difference in the numerator and denominator isotopes for a particular isotope ratio. For example, if $m_j = 56$, $a_X = +2$, $a_Y = -2$, and $a_Z = +1$, where $X = {}^{58}Fe/{}^{56}Fe$, $Y = {}^{54}Fe/{}^{56}Fe$, and $Z = {}^{57}Fe/{}^{56}Fe$. Eq. (1) produces a straight line on a plot of two measured (fractionated) isotope ratios, such as X_U^M versus Y_U^M or X_U^M versus Z_U^M.

However, another commonly used "linear" mass fractionation law has the form

$$X_U^T = X_U^M(1 + a_X f_1) \tag{3}$$

(e.g. [26]; isotope ratios are defined above; f_1 is the mass fractionation factor per mass). Assuming an analogous relation for isotope ratio Y, Eq. (3) does not produce a straight line on a plot of two measured (fractionated) isotope ratios, such as X_U^M versus Y_U^M, although it is a common misconception that this is the case. This is easily seen by rearranging Eq. (3) so that X_U^M is the dependent variable, or casting Eq. (3) in the Hart and Zindler [27] form. To distinguish the above mentioned two mass fractionation laws, we refer to Eq. (1) as true linear mass fractionation and Eq. (3) as a linear form for mass fractionation, recognizing that the latter does not describe a straight line on a plot of X_U^M versus Y_U^M or X_U^M versus Z_U^M.

It is now well accepted that instrumentally produced mass fractionation of intermediate-mass elements follows an exponential form [3,24,26,27]. Solution of the double-spike problem by using a true exponential mass fractionation law is not possible due to the transcendental nature of the combined equations. However, as noted by Russell et al. [3], the exponential mass fractionation law may be approximated through a series expansion. Expansion to the first-order produces

$$X_U^T = X_U^M\left(1 + f_1 m_{i-j}^X - f_1 \frac{[m_{i-j}^X]^2}{2m_j}\right) \tag{4}$$

which is essentially the linear form [Eq. (3)] with a modification of the mass-difference coefficients, where

$$a_X = m_{i-j}^X - \frac{[m_{i-j}^X]^2}{2m_j}, \qquad a_Y = m_{i-j}^Y - \frac{[m_{i-j}^Y]^2}{2m_j},$$

$$a_Z = m_{i-j}^Z - \frac{[m_{i-j}^Z]^2}{2m_j} \tag{5}$$

Higher-order expansions of the exponential law no longer follow the simple functional form of Eq. (3), which prevents reasonable simultaneous solution (in the following). We refer to Eq. (4) as an *exponential approximation*.

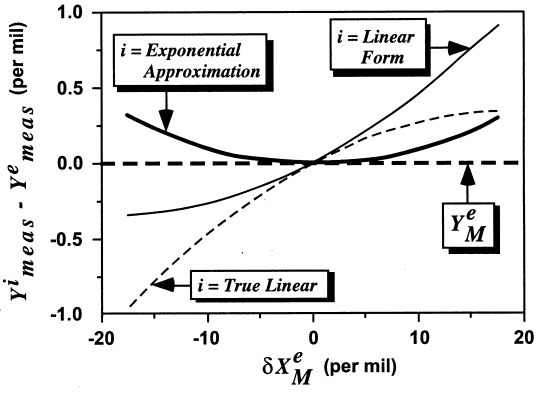

Fig. 2. Deviations in various mass fractionation laws as compared to exponential mass fractionation. δX^e_{meas} is defined as the per mil deviation in the measured $^{58}Fe/^{56}Fe$ ratio, relative to the true (not fractionated) ratio, as theoretically generated using exponential mass fractionation and a β of $+0.5$ to -0.5 (e.g. [3]); the majority of measured (fractionated) $^{58}Fe/^{56}Fe$ ratios using TIMS fall within the range of ± 10 per mil. $Y^i_{\text{meas}} - Y^e_{\text{meas}}$ is defined as the per mil difference in the measured $^{54}Fe/^{56}Fe$ ratio calculated using a given fractionation law i, relative to that calculated assuming exponential mass fractionation, at a given δX^e_{meas} value. Both true linear mass fractionation [Eq. (1)] and fractionation that follows a linear form [Eq. (3)] deviate significantly from exponential mass fractionation over the range of measured (fractionated) Fe isotope ratios, which introduces large errors in double-spike solutions that assume such fractionation corrections (e.g. [15,19,21]). Exponential mass fractionation can be closely approximated using a first-order series expansion of the exponential equation [Eqs. (4) and (5)], which can be considered a modification of the linear form, and this approach is followed here.

Using our *exponential approximation* [Eq. (4)] for the mass fractionation law introduces an error of less than 0.1 per mil in, e.g. the $^{54}Fe/^{56}Fe$ ratio, over the range of instrumental fractionation that we measure and assuming that the true instrumentally produced mass fractionation follows an exponential law (Fig. 2). However, if true linear mass fractionation [Eq. (1)] or the linear form [Eq. (3)] is used, the errors introduced are on the order of 1 per mil in the $^{54}Fe/^{56}Fe$ ratio, over the range of instrumental fractionation that we measure and assuming that the true instrumentally produced mass fractionation follows an exponential law (Fig. 2). Such large errors will obliterate most of the isotopic variations seen in

nature for Fe [23–25]. Therefore, solutions to the double-spike method that assume either true linear mass fractionation [Eq. (1)] (e.g. [19]) or the linear form for mass fractionation [Eq. (3)] (e.g. [15]), will have very large propagated errors if the measured data follow an exponential law. In the error analysis presented below, use of the exponential approximation [Eq. (4)] accounts for only 5%–10% of the total error in the final calculations, assuming instrumental mass fractionation follows an exponential law.

3. General derivation of the double-spike solution

The fractionation curve for the unspiked sample (unknown) (curve U in Fig. 1) is described by

$$X_U^T = X_U^M(1 + a_X f_1), \qquad Y_U^T = Y_U^M(1 + a_Y f_1),$$
$$Z_U^T = Z_U^M(1 + a_Z f_1) \tag{6}$$

where f_1 is the mass fractionation factor for the sample (unknown), and a_X, a_Y, and a_Z are the mass-difference coefficients, as modified by the exponential approximation [Eq. (5)], and isotope ratios X, Y, and Z are defined previously.

The fractionation curve for the mixture (spike + sample) (curve M in Fig. 1) is described by

$$X_M^T = X_M^M(1 + a_X f_2), \quad Y_M^T = Y_M^M(1 + a_Y f_2),$$
$$Z_M^T = Z_M^M(1 + a_Z f_2) \tag{7}$$

where f_2 is the mass fractionation factor for the mixture (spike + sample).

The line that connects the true isotopic compositions of the sample, mixture, and spike (line UMS in Fig. 1) is given by

$$X_M^T = X_U^T + h(X_S - X_U^T),$$
$$Y_M^T = Y_U^T + h(Y_S - Y_U^T),$$
$$Z_M^T = Z_U^T + h(Z_S - Z_U^T) \tag{8}$$

where h is the parameter for the parametric equation form of line UMS, and X_S, Y_S, and Z_S are the true isotopic compositions of the spike, for isotope ratios X, Y, and Z, respectively.

Because the isotope ratios X, Y, and Z may be defined as m_i/m_j, where m_i is a variable and m_j is a constant for a given set of isotope ratios, we may define three sets of ratios, which produce three sets of double-spike solutions. In the case of Fe, for $m_j = 56$ ("56-based solutions"), we define $X = {}^{58}\text{Fe}/{}^{56}\text{Fe}$, $Y = {}^{54}\text{Fe}/{}^{56}\text{Fe}$, and $Z = {}^{57}\text{Fe}/{}^{56}\text{Fe}$ (Fig. 1). For $m_j = 54$ ("54-based solutions"), we define $X = {}^{56}\text{Fe}/{}^{54}\text{Fe}$, $Y = {}^{57}\text{Fe}/{}^{54}\text{Fe}$, and $Z = {}^{58}\text{Fe}/{}^{54}\text{Fe}$. For $m_j = 57$ ("57-based solutions"), we define $X = {}^{54}\text{Fe}/{}^{57}\text{Fe}$, $Y = {}^{56}\text{Fe}/{}^{57}\text{Fe}$, and $Z = {}^{58}\text{Fe}/{}^{54}\text{Fe}$. Because of the very small abundance of ${}^{58}\text{Fe}$, we do not define a set of ratios with $m_j = 58$.

Although we present the graphical illustration of Hofmann [19] in Fig. 1, our derivation is quite different; Hofmann used a true linear mass fractionation law [Eq. (1)], which introduces large errors (many per mil) in the double-spike solutions when instrumental mass fractionation follows the exponential or linear form laws. The double-spike solutions of Gale [15] and Hamelin et al. [21] use a linear form for mass fractionation [Eq. (3)], which can be recast to approximate exponential mass fractionation, but Gale's solution is only given for Pb, and Hamelin et al. do not provide their solutions.

Equations (6), (7), and (8) are arranged for solution of the nine unknowns, X_U^T, Y_U^T, Z_U^T, X_M^T, Y_M^T, Z_M^T, f_1, f_2, and h. Combining these sets produces

$$X_U^M(1 + a_X f_1)(1 - h) + hX_S = X_M^M(1 + a_X f_2) \tag{9}$$

$$Y_U^M(1 + a_Y f_1)(1 - h) + hY_S = Y_M^M(1 + a_Y f_2) \tag{10}$$

$$Z_U^M(1 + a_Z f_1)(1 - h) + hZ_S = Z_M^M(1 + a_Z f_2) \tag{11}$$

Solution of Eq. (9)–(11) produces a solution for f_1, the primary parameter of interest:

$$f_1 = \frac{a_Z Z_M^M A + a_Y Y_M^M B + a_X X_M^M C}{a_Y a_Z (X_M^M - X_S)(Y_U^M Z_M^M - Y_M^M Z_U^M) + a_X D} \tag{12}$$

where

$$A = X_S(Y_U^M - Y_M^M) + Y_S(X_M^M - X_U^M) + X_U^M Y_M^M - X_M^M Y_U^M$$

Table 2
Parameters for error propagation calculations[a]

Solution set	X_U^M	Y_U^M	Z_U^M	X_M^M	Y_M^M	Z_M^M
$m_j = 56$	$^{58}Fe/^{56}Fe$	$^{54}Fe/^{56}Fe$	$^{57}Fe/^{56}Fe$	$^{58}Fe/^{56}Fe$	$^{54}Fe/^{56}Fe$	$^{57}Fe/^{56}Fe$
	± 0.1%	± 0.025%	± 0.025%	± 0.2%	± 0.01%	± 0.02%
$m_j = 54$	$^{56}Fe/^{54}Fe$	$^{57}Fe/^{54}Fe$	$^{58}Fe/^{54}Fe$	$^{56}Fe/^{54}Fe$	$^{57}Fe/^{54}Fe$	$^{58}Fe/^{54}Fe$
	± 0.025%	± 0.025%	± 0.1%	± 0.01%	± 0.02%	± 0.02%
$m_j = 57$	$^{54}Fe/^{57}Fe$	$^{56}Fe/^{57}Fe$	$^{58}Fe/^{57}Fe$	$^{54}Fe/^{57}Fe$	$^{56}Fe/^{57}Fe$	$^{58}Fe/^{57}Fe$
	± 0.025%	± 0.025%	± 0.1%	± 0.02%	± 0.02%	± 0.02%

[a] Error propagation illustrated in Figs. 3 and 4 are the average one standard deviation errors calculated for X_U^T, Y_U^T, and Z_U^T, on a per-mass basis (i.e. the error calculated for the $^{54}Fe/^{56}Fe$ ratio is divided by 2, etc.), using 1000 randomly generated values for (X_U^M, Y_U^M, Z_U^M) and (X_M^M, Y_M^M, Z_M^M) assuming exponential mass fractionation ($\beta = -0.5$ to $+0.5$, which matches the average measured range), and randomly assigned errors for the isotope ratios within the limits below. The assigned errors match those estimated for the measured ratios based on the external precision for standards that have been corrected for mass fractionation using internal normalization.

$$B = X_S(Z_M^M - Z_U^M) + Z_S(X_U^M - X_M^M) + X_M^M Z_U^M - X_U^M Z_M^M$$

$$C = Y_S(Z_U^M - Z_M^M) + Z_S(Y_M^M - Y_U^M) + Y_U^M Z_M^M - Y_M^M Z_U^M$$

$$D = a_Y(Z_M^M - Z_S)(X_U^M Y_M^M - X_M^M Y_U^M) - a_Z(Y_M^M - Y_S) \cdot (X_U^M Z_M^M - X_M^M Z_U^M)$$

Note that these are not coefficients of a plane, but are simply used for convenience.

It is also useful to calculate the spike to sample ratio, which is obtained through solution for the parameter h by using Eqs. (9)–(11):

$$h = \frac{-a_Y a_Z A_h + a_X(-a_Y B_h + a_Z C_h)}{-a_Y a_Z D_h + a_X(-a_Y E_h + a_Z F_h)} \quad (13)$$

where

$$A_h = (X_M^M - X_U^M)(Y_U^M Z_M^M - Y_M^M Z_U^M)$$

$$B_h = (Z_M^M - Z_U^M)(X_U^M Y_M^M - X_M^M Y_U^M)$$

$$C_h = (Y_M^M - Y_U^M)(X_U^M Z_M^M - X_M^M Z_U^M)$$

$$D_h = (X_S - X_U^M)(Y_U^M Z_M^M - Y_M^M Z_U^M)$$

$$E_h = (Z_S - Z_U^M)(X_U^M Y_M^M - X_M^M Y_U^M)$$

$$F_h = (Y_S - Y_U^M)(X_U^M Z_M^M - X_M^M Z_U^M)$$

h is related to the sample to spike ratio by

$$h = \left(1 + \frac{M_U}{M_S}\frac{\mathrm{Ab}_U^{mj}}{\mathrm{Ab}_S^{mj}}\right)^{-1} \quad (14)$$

where M_U and M_S are the moles of sample (unknown) and spike, respectively, and Ab_U^{mj} and Ab_S^{mj} is the abundance of mass m_j in the sample (unknown) and spike, respectively (i.e. $m_j = 56$ for $X = {}^{58}Fe/{}^{56}Fe$, $Y = {}^{54}Fe/{}^{56}Fe$, and $Z = {}^{57}Fe/{}^{56}Fe$). Note that the weights of the spike and sample are not required in the solution. If the abundances of m_j in the sample (unknown) and spike are known, the sample to spike ratio may be directly calculated from h. Dodson [18] assumed that h (he defines as P_K) is directly equal to the spike to sample ratio in his solution to the double-spike problem, an assumption that introduces significant errors at the per mil level of precision.

Error propagation: Although rigorous correction for instrumental mass fractionation can be made by using the double-spike technique, error amplification can produce uncertainties in the corrected ratios that are up to or exceed by an order of magnitude the errors that would be produced using the same measured data and internal normalization. The amount of error amplification is strongly dependent upon the isotopic composition of the spike and the spike to sample ratio in the mixture aliquot, and here we present an analysis of the optimum spike isotope composition for Fe isotope analysis (see also Table 2).

The precision of the true isotopic ratios of the unspiked aliquot are in part controlled by the angle

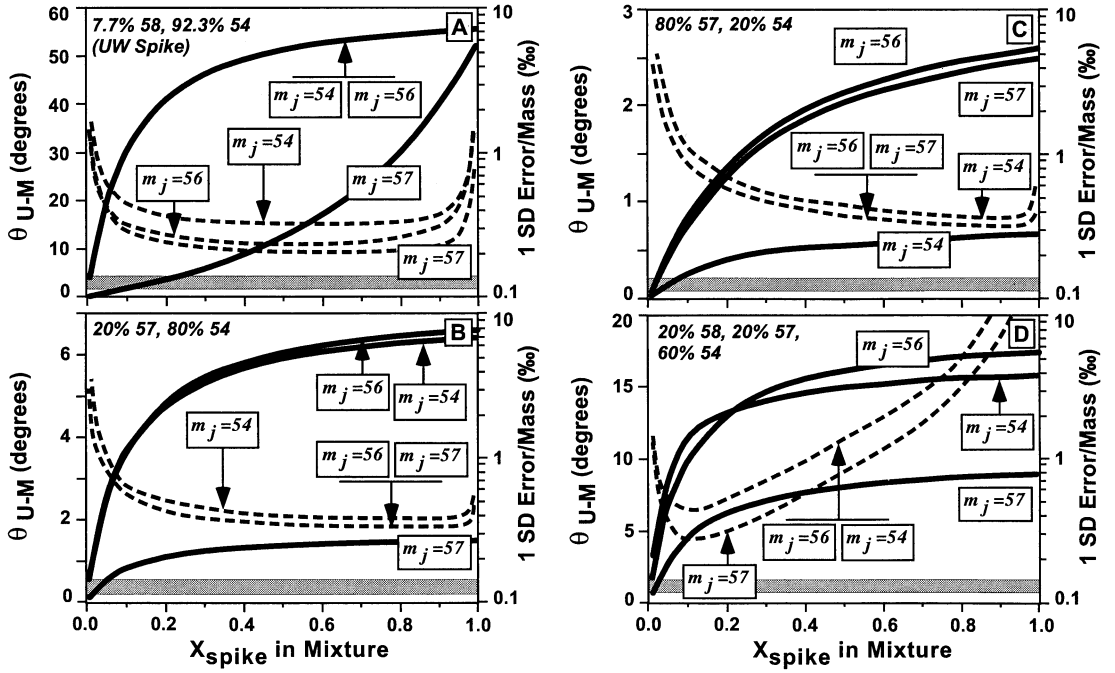

Fig. 3. Example geometric relations and calculated error propagation for double and triple spikes for Fe isotopes. X_{spike} is the mole fraction of spike in the mixture. Heavy solid lines indicate the variations in θ_{U-M}, the angle between the unknown and mixture fractionation lines (Fig. 1), as a function of the fraction of spike in the mixture. Dashed lines indicate the per mil errors (1 standard deviation) in calculated true isotope ratios X_U^T, Y_U^T, Z_U^T, on a per-mass basis, as a function of the fraction of spike in the mixture, using the parameters in Table 2. Calculated errors assume errors in both the unknown and mixture measurements (Table 2). Synthetically generated measured ratios are assumed to fractionate following an exponential law, and data are corrected using the exponential approximation [Eqs. (4) and (5)]. Three sets of double-spike solutions can be written, each with a distinct denominator isotope (m_j). For $m_j = 56$, we define $X = {}^{58}\text{Fe}/{}^{56}\text{Fe}$, $Y = {}^{54}\text{Fe}/{}^{56}\text{Fe}$, and $Z = {}^{57}\text{Fe}/{}^{56}\text{Fe}$ (Fig. 1). For $m_j = 54$, we define $X = {}^{56}\text{Fe}/{}^{54}\text{Fe}$, $Y = {}^{57}\text{Fe}/{}^{54}\text{Fe}$, and $Z = {}^{56}\text{Fe}/{}^{54}\text{Fe}$. For $m_j = 57$, we define $X = {}^{54}\text{Fe}/{}^{57}\text{Fe}$, $Y = {}^{56}\text{Fe}/{}^{57}\text{Fe}$, and $Z = {}^{58}\text{Fe}/{}^{57}\text{Fe}$. In all cases, as the fraction of spike decreases below 0.1, propagated errors increase dramatically, in part reflecting the decrease in the angle θ_{U-M}. In general, errors are lowest when θ_{U-M} is greatest, although θ_{U-M} is not the sole contributor to the errors. The most robust double-spike solutions will involve a spike that produces low errors over a range of X_{spike} in the mixtures. The gray bar indicates the measured per mil error for our Fe standard using the U.W. Madison ${}^{58}\text{Fe}$–${}^{54}\text{Fe}$ spike and assuming a constant reference ratio for the double-spike calculation (see text). (A) Calculations using the U.W. mixed ${}^{58}\text{Fe}$–${}^{54}\text{Fe}$ spike (7.7% ${}^{58}\text{Fe}$, 92.3% ${}^{54}\text{Fe}$). (B) Calculations using a mixed ${}^{57}\text{Fe}$–${}^{54}\text{Fe}$ spike (20% ${}^{57}\text{Fe}$, 80% ${}^{54}\text{Fe}$). (C) Calculations using a mixed ${}^{57}\text{Fe}$–${}^{54}\text{Fe}$ spike (80% ${}^{57}\text{Fe}$, 20% ${}^{54}\text{Fe}$). (D) Calculations using a mixed ${}^{58}\text{Fe}$–${}^{57}\text{Fe}$–${}^{54}\text{Fe}$ spike (20% ${}^{58}\text{Fe}$, 20% ${}^{57}\text{Fe}$, 60% ${}^{54}\text{Fe}$).

θ_{U-M}, which is the intersection angle between the unknown and mixture fractionation curves, as viewed down the mixing line *UMS* (inset; Fig. 1). As the angle between the two fractionation curves decreases, either due to decreasing the spike to sample ratio or changing the isotopic composition of the spike, calculation of the true isotopic composition of the unknown aliquot can be subject to large errors (Fig. 3); this general effect was noted by Hamelin et al. [21]. In all cases, at low spike to sample ratios, the nearly coincident mass fractionation curves *U* and *M* (Fig. 1) produce large errors in the corrected ratios for the unknown (Fig. 3). Conversely, although θ_{U-M} is greatest at high spike to sample ratios, the true isotopic composition of the unknown is poorly determined because of the large extrapolation of the line *UMS* (Figs. 1 and 3). The smallest amount of error propagation tends to occur when the choice of spike produces θ_{U-M} greater than 10° (Fig. 3). The most robust double-spike results are produced when a spike isotope composition is chosen that produces propagated errors which are low and relatively constant

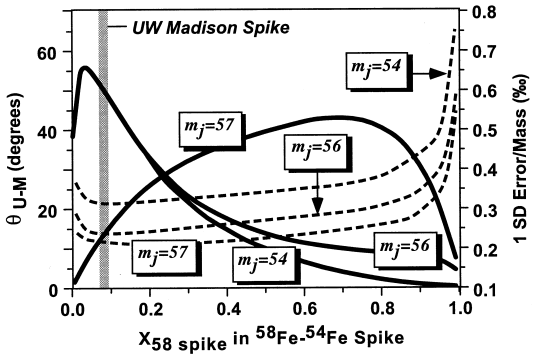

Fig. 4. Geometric and error relations for an ^{58}Fe–^{54}Fe double spike. $X_{58\ spike}$ is the mole fraction of ^{58}Fe spike in the ^{58}Fe–^{54}Fe double spike. Heavy solid lines indicate the variations in θ_{U-M}, the angle between the unknown and mixture fractionation lines (Fig. 1), as a function of $X_{58\ spike}$. Dashed lines indicate the per mil errors (1 standard deviation) in calculated true isotope ratios X_U^T, Y_U^T, Z_U^T, on a per-mass basis, as a function of $X_{58\ spike}$, using the parameters in Table 2. Calculated errors assume errors in both the unknown and mixture measurements (Table 2). Synthetically-generated measured ratios are assumed to fractionate following an exponential law, and data are corrected using the exponential approximation [Eq. (4)]. The fraction of the ^{58}Fe–^{54}Fe double spike in the mixture is set at 0.5 (X_{spike}). As noted in Fig. 3, three sets of double-spike solutions can be written, each with a distinct denominator isotope (m_j); curves are shown for m_j = 56 (see Fig. 1), m_j = 54, and m_j = 57. In all cases, as $X_{58\ spike}$ decreases below 0.05 or exceeds 0.9, propagated errors increase dramatically. The generally increasing error with increasing $X_{58\ spike}$ (above $X_{58\ spike}$ = 0.2) in part reflects the decrease in the angle θ_{U-M} for the solution sets m_j = 56 and m_j = 54. The U.W. Madison ^{58}Fe–^{54}Fe double spike (7.7% ^{58}Fe, 92.3% ^{54}Fe) lies near the minimum for propagated errors for all three solution sets.

over a reasonable range of X_{spike} (fraction of spike in the mixture), generally between X_{spike} = 0.2–0.8 [Fig. 3(A)].

Error analysis of a variety of double and triple spikes indicates that, for Fe, the lowest propagated errors are produced with a mixed ^{58}Fe–^{54}Fe spike [Fig. 3(A)]. Small, but significant variations in error propagation are produced over the possible range of spike compositions for an ^{58}Fe–^{54}Fe spike. Propagated errors are lowest for an ^{58}Fe–^{54}Fe spike that is composed of ~10% ^{58}Fe and ~90% ^{54}Fe (Fig. 4), which is close to the isotopic composition of the U.W. Madison mixed ^{58}Fe–^{54}Fe spike (see Table 4).

In its most general application, where the isotopic composition of the sample is completely unknown, the double-spike procedure requires analysis of an unspiked aliquot and a spiked aliquot. This approach must be taken, for example, in the case of Pb isotope analysis, because Pb isotope ratios in natural samples are not predictably correlated, being functions of age and U/Pb and Th/Pb ratios. However, if isotopic variations are only a result of naturally occurring, mass-dependent fractionation, the unspiked aliquot does not need to be measured for each sample, once the natural isotopic variation of a particular reservoir is characterized (e.g. [3]). This simplification is robust and will not produce any bias in the results unless (1) the natural-occurring mass fractionation is very large and follows a different mass-dependent fractionation law from that used to correct instrumental mass fractionation (e.g. linear law versus Rayleigh distillation), and (2) the unknown sample does not lie on the natural fractionation curve of the assumed reservoir. The first factor is entirely negligible for natural isotope variations on the order of several per mil. The second factor may be significant for different planetary bodies or nucleosynthetic reservoirs; this is perhaps best illustrated for oxygen isotopes, where terrestrial and lunar samples lie on an ^{18}O/^{16}O–^{17}O/^{16}O natural fractionation array that is distinct from that of some meteorite components or the planet Mars [28].

The validity of only analyzing the mixture when all natural compositions lie on the same natural fractionation line can be visualized in Fig. 1 (inset); it is the mixture curve (curve *M*) that determines the intersection of line *UMS* with the natural fractionation curve (curve *U*), if curve *U* is known. Application of the "mixture-only" approach increases the precision of the corrected ratios by approximately a factor of 2, because error propagation is not dependent on errors associated with measurement of the unspiked aliquot. In the case of Fe isotopes, this approach is a significant advantage because the most difficult mass of Fe to analyze in the unspiked aliquot is ^{58}Fe due to its low abundance and isobaric interferences by ^{58}Ni, as well as the fact that natural isotopic variations are small. Errors associated with analysis of ^{58}Fe in the mixture aliquot are significantly less when using an ^{58}Fe–^{54}Fe spike because of the increased abundance of ^{58}Fe in the mixture.

Table 3
Collector configuration used for static multicollector analysis of Fe isotope ratios[a]

	Low 2	Low 1	Axial	High 1	High 2	High 3	High 4
Background	51.5	52.5	53.5	54.5	55.5		56.5
Scan 1	^{52}Cr		^{54}Fe		^{56}Fe		
Scan 2		^{56}Fe	^{57}Fe	^{58}Fe			^{60}Ni

[a] The Micromass Sector 54 collector block is designed for a working range in mass spread of 9.5%. To simultaneously analyze all four Fe isotopes and continuously monitor for Cr and Ni isobars would require a relative mass spread of 14.4%. Therefore, two multicollection scans are used. A beam growth correction using the ion intensity measured for ^{56}Fe in scans 1 and 2 is used for measurement of the ^{54}Fe/^{57}Fe and ^{54}Fe/^{58}Fe ratios.

Absolute uncertainties in the spike isotope composition do not affect the precision of the double-spike solutions, but do affect the absolute values of the corrected Fe isotope composition of the unknown. The confidence of relative differences in isotopic compositions for samples is therefore unaffected by the absolute uncertainty of the spike. The accuracy of absolute Fe isotope ratios for a sample, however, is linearly related to the accuracy of the spike isotopic composition; a one per mil/mass shift in the spike isotopic composition produces a one per mil/mass shift in the sample isotopic composition (although the relative isotopic difference between samples is unaffected). We estimate that the absolute uncertainty in the isotopic composition of our spike is 2%–3‰ per mass, and the absolute uncertainty of our measurements will be equal to this range. The linear relation between accuracy of the absolute isotope compositions of the sample and that of the spike is independent of the spike to sample ratio.

4. Mass analysis of Fe

All isotope analyses were conducted at the University of Wisconsin Radiogenic Isotope Laboratory using a Mircomass Sector 54 TIMS mass spectrometer. This instrument is fitted with seven Faraday collectors and an analog Daly detector. Filament ribbon used for Fe isotope analysis is 99.999% pure ("zone-refined") Re and is 0.0010 in. thick by 0.030 in. wide. After adding an Al_2O_3 slurry to a single blank filament, the Fe sample (~4 μg of Fe) is loaded, followed by 1 *M* H_3PO_4, followed by silica gel. This loading recipe was chosen after evaluating the boric acid–silica gel technique [6,8,10]. The Al_2O_3 slurry emitter produces longer lasting and more stable ion beams and high ion currents ($>2 \times 10^{-11}$ A total current) as compared to the boric acid–silica gel technique [29].

Mass analysis of Fe uses a two-scan multicollector routine, in addition to a background scan, that monitors interferences caused by ^{54}Cr and ^{58}Ni, using ^{52}Cr and ^{60}Ni, respectively (Table 3). Corrections for these isobars are made using ^{54}Cr/^{52}Cr = 0.0282 and ^{58}Ni/^{60}Ni = 2.616. The ^{54}Cr correction on ^{54}Fe is typically 0.002% at the beginning of the analysis and drops to 0 by the end of the analysis. To avoid adding noise to the data we do not use Ni-corrected ratios unless the ^{60}Ni ion intensity average for a block is $>9 \times 10^{-17}$ A. This threshold was chosen by evaluating the ^{58}Fe/^{56}Fe ratio measured for unspiked Johnson-Mathey (J-M) Fe standard data; it produces the lowest external standard deviation measurement for the ^{58}Fe/^{56}Fe measurement. We note that Ni isobaric corrections were at most a 0.01% correction. Nickel isobaric interferences, when present, burned off during the course of the run, and only 10% of the analyses made required Ni isobaric corrections.

5. Precision of Fe isotope measurements

Our lab standard is a J-M Fe standard, and this can be measured to a precision of ±0.26 per mil (1 SD) for the ^{54}Fe/^{56}Fe ratio, using 21 analyses of 12 mixtures (X_{spike} = 0.13–0.38; Table 4). Using the average ratios (when available) of mixtures that have

Table 4
Corrected iron isotope compositions of the UW mixed ^{54}Fe–^{58}Fe double spike and the J-M Fe standard[a]

	$^{54}Fe/^{56}Fe$	Error	$^{57}Fe/^{56}Fe$	Error	$^{58}Fe/^{56}Fe$	Error	$\delta^{56}Fe$ ‰	Error ‰	Frac spike in mix
UW mixed ^{54}Fe–^{58}Fe spike									
	34.598	±39	0.068 788	±78	2.419 7	±29			
J-M ultra pure Fe standard									
Mix 1	0.063 646	±8	0.023 094	±1	0.003 063 1	±4	0.59	0.13	0.373
	0.063 714	±18	0.023 082	±3	0.003 060 0	±8	−0.49	0.28	0.373
Mix 2	0.063 664	±7	0.023 091	±1	0.003 062 3	±3	0.29	0.11	0.133
Mix 3	0.063 707	±16	0.023 083	±3	0.003 060 3	±7	−0.38	0.24	0.310
	0.063 660	±9	0.023 091	±2	0.003 062 4	±4	0.35	0.14	0.310
Mix 4	0.063 672	±11	0.023 089	±2	0.003 061 9	±5	0.17	0.17	0.187
	0.063 719	±14	0.023 081	±2	0.003 059 9	±7	−0.56	0.22	0.187
Mix 5	0.063 669	±12	0.023 090	±2	0.003 062 1	±6	0.23	0.19	0.191
Mix 6	0.063 679	±16	0.023 088	±3	0.003 061 6	±7	0.07	0.25	0.183
	0.063 669	±15	0.023 090	±3	0.003 062 1	±7	0.23	0.23	0.183
Mix 7	0.063 677	±10	0.023 088	±2	0.003 061 7	±5	0.10	0.15	0.237
	0.063 676	±10	0.023 089	±2	0.003 061 7	±5	0.10	0.16	0.237
Mix 8	0.063 694	±10	0.023 085	±2	0.003 060 9	±4	−0.18	0.15	0.213
	0.063 647	±12	0.023 094	±2	0.003 063 0	±6	0.56	0.20	0.213
Mix 9	0.063 686	±17	0.023 087	±3	0.003 061 3	±8	−0.05	0.27	0.193
	0.063 667	±12	0.023 090	±2	0.003 062 1	±6	0.25	0.19	0.193
Mix 10	0.063 680	±13	0.023 088	±2	0.003 061 5	±6	0.04	0.20	0.164
Mix 11	0.063 676	±9	0.023 089	±2	0.003 061 7	±4	0.10	0.14	0.242
	0.063 687	±15	0.023 087	±3	0.003 061 2	±7	−0.07	0.23	0.242
Mix 12	0.063 669	±9	0.023 090	±2	0.003 062 0	±4	0.22	0.15	0.379
	0.063 695	±8	0.023 085	±1	0.003 060 8	±4	−0.19	0.13	0.379
Average	0.063 679	±19	0.023 088	±3	0.003 061 6	±8	0.06	0.29	

[a] The composition of the UW mixed ^{54}Fe–^{58}Fe is the average of 4 analyses. The quoted errors are one standard deviation of the mean based on internal normalization of the data to the average measured $^{54}Fe/^{57}Fe$ ratio. Errors for the J-M Fe standard are one standard error as calculated by individual block analyses of the mixture aliquot. The different mixes for the J-M Fe standard analyses refer to differing spike to sample ratios in the mixture aliquot (Frac spike in mix column); each analysis is a separate filament load. Errors for the average J-M Fe standard are one standard deviation. The J-M Fe standard was prepared from 1 g of ultrapure Fe rod purchased from Johnson Matthey chemicals, Lot # 010785.

been run in duplicate produces a precision of ±0.12 per mil (1 SD) for the $^{54}Fe/^{56}Fe$ ratio. There is no correlation between the calculated true isotopic composition of the standard with that of the fraction of spike in the mixture (Fig. 5), confirming the robustness of the double-spike corrections. Overall, calculations using $m_j = 56$ or 57 produce similar results and errors, as expected from the error propagation models (Figs. 3 and 4); solutions based on $m_j = 54$ produced similar results but the spread in repeat analyses was greater as compared to solutions using $m_j = 56$ or 57. Eighteen of the analyses yielded solutions for $m_j = 54$ or 57 that were between 0.1 and 0.3 per mil/mass of the solutions using $m_j = 56$. The analyses that produced different solutions using $m_j = 56$, 57, or 54 were typically associated with unstable ion beams. Although error propagation suggests that $m_j = 57$ solutions should be the most precise (Figs. 3 and 4), we believe that the imprecision of the $m_j = 57$ and 54 solutions are largely a reflection of the two-scan multicollector routine used to analyze the Fe mass spectrum, because ion beam fluctuations are likely to cause imprecision of the measurements for $^{54}Fe/^{57}Fe$ and $^{58}Fe/^{54}Fe$ ratios, which cannot be measured in a single scan (Table 3).

The average of 21 analyses of the J-M Fe standard

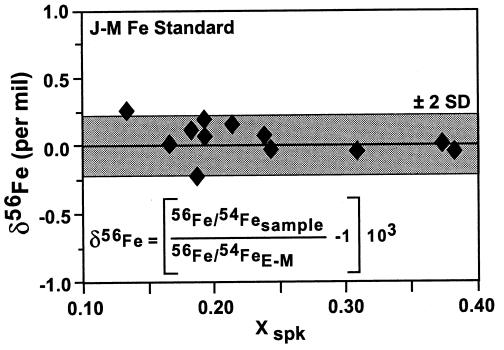

Fig. 5. Calculated δ^{56}Fe values of the J-M Fe standard, using a range of spike fractions in the mixture (X_{spike}). Symbols are averages of the 12 mixtures in Table 4. There is no bias in the calculated true isotope composition over this range of spike fractions, demonstrating the robustness of the double spike correction. Error envelope is the two standard deviation of the averages of the 12 mixtures (Table 4).

is $^{54}Fe/^{56}Fe = 0.063\,679 \pm 19$ (1 SD), $^{57}Fe/^{56}Fe = 0.023\,088 \pm 3$, $^{58}Fe/^{56}Fe = 0.003\,061\,6 \pm 8$ (Table 4). Isotopic analysis of a wide variety of igneous rocks yields $^{54}Fe/^{56}Fe = 0.063\,685 \pm 16$ (1 SD), $^{57}Fe/^{56}Fe = 0.023\,087 \pm 3$, $^{58}Fe/^{56}Fe = 0.003\,061\,3 \pm 7$ ($n = 20$) [24], which is indistinguishable from the isotopic composition of J-M Fe. We therefore combine the data sets to define a bulk Earth-Moon Fe isotope composition of $^{54}Fe/^{56}Fe = 0.063\,683 \pm 17$ (1 SD), $^{57}Fe/^{56}Fe = 0.023\,087 \pm 3$; and $^{58}Fe/^{56}Fe = 0.003\,061\,4 \pm 8$. By using this bulk Earth-Moon (E-M) composition as a reference, we define:

$$\delta^{56}Fe = ([^{56}Fe/^{54}Fe]_{sample}/[^{56}Fe/^{54}Fe]_{E\text{-}M} - 1) \times 10^3 \quad (15)$$

We use the inverse of the measured $^{54}Fe/^{56}Fe$ ratio to follow the convention of stable isotope measurements, which define δ values for isotope ratio variations as "heavy over light" masses. Use of a different set of isotope ratios such as the $^{57}Fe/^{54}Fe$ or $^{58}Fe/^{54}Fe$ are equally valid, and although use of these ratios would produce larger variations in δ values because the mass difference is larger, the errors associated with these corrected values are proportionally larger using the double-spike approach. This is also true for the empirical approach [10].

The accuracy of our reported Fe isotope ratios are excellent as compared to the iron isotope ratios reported by Taylor et al. [11] and Walczyk [12]; the $^{54}Fe/^{56}Fe$ ratio determined in this study is within 0.2 and 1 per mil, respectively, of the $^{54}Fe/^{56}Fe$ ratio reported by these workers. In contrast, the $^{54}Fe/^{56}Fe$ measurements reported by Dixon et al. [10] differ by 5 per mil, despite the fact that they used the gravimetric standards of Taylor et al. [11]. The cause of the significant differences between our Fe isotope ratio measurements and those of Dixon et al. [10] are unexplained but may be due to the low-level detection method used by Dixon et al. [10], in comparison to the use of Faraday collectors by Taylor et al. [11], Walczyk [12], and this study.

6. Conclusions

Instrumentally produced mass fractionation in a thermal ionization mass spectrometer may be rigorously corrected using the double-spike approach. The closed-form derivation we present is completely general, being applicable to any element with four or more isotopes, and provides an excellent approximation to exponential mass fractionation in the TIMS source, over the range of measured instrumentally produced mass fractionation. In addition, it is shown that the spike isotope composition has a significant effect on the error propagation of the double-spike approach. In the case of Fe isotope measurements, a spike of ~10% ^{58}Fe and 90% ^{54}Fe minimizes propagated uncertainties. This approach has produced the highest precision Fe isotope ratios reported to date, on the order of ±0.2–0.3 per mil for the $^{54}Fe/^{56}Fe$ ratio, while preserving natural isotope variations in samples. Our approach utilizes all Fe isotope ratios, which is important for assessing data quality. In addition, Fe isotope geochemistry is just emerging as a new discipline, and it is as yet unknown if all terrestrial or extraterrestrial samples lie on the same mass fractionation lines; this can only be assessed by analyzing all Fe isotope ratios. Although other instrumentation such as ICP-MS offers higher ionization efficiency for Fe as compared to TIMS, ArN^+ and ArO^+ interferences present significant difficulties in obtaining high-

precision isotope analyses of all isotope ratios using current ICP-MS technology.

Acknowledgements

This research was supported by NSF grant no. OPP-9713968 and NASA grant no. NAG5-6342, and the NASA Astrobiology Institute. We thank Herb Wang and Zulcas Baumgartner for helpful discussions.

References

[1] J. Hoefs, Stable Isotope Geochemistry, Springer Verlag, New York, 1987.
[2] A.P. Dickin, Radiogenic Isotope Geology, Cambridge University Press, Cambridge, 1995.
[3] W.A. Russell, D.A. Papanastassiou, T.A. Tombrello, Geochim. Cosmochim. Acta 42 (1978) 1075.
[4] J. Skulan, D.J. DePaolo, T.L. Owens, Geochim. Cosmochim. Acta 61 (1997) 2505.
[5] Z. Peng, J.D. Macdougall, Geochim. Cosmochim. Acta 62 (1998) 1691.
[6] A. Götz, K.G. Heumann, Int. J. Mass Spectrom. Ion Processes 83 (1988) 319.
[7] I.D. Hutcheon, J.T. Armstrong, G.J. Wasserburg, Geochim. Cosmochim. Acta 51 (1987) 3175.
[8] J. Völkening, D.A. Papanastassiou, Astrophys. J. 347 (1989) L43.
[9] P.R. Dixon, D.R. Janecky, R.E. Perrin, D.J. Rokop, P.L. Unkefer, W.D. Spall, R. Maeck, Unconventional Stable Isotopes: Iron, Y.K. Kharaka and A.S. Maest (Eds.), A.A. Balkema, Rotterdam, The Netherlands, 1992, Vol. 2, pp. 915–918.
[10] P.R. Dixon, R.E. Perrin, D.J. Rokop, R. Maeck, D.R. Janecky, J.P. Banar, Anal. Chem. 65 (1993) 2125.
[11] P.D.P. Taylor, R. Maeck, P. De Bièvre, Int. J. Mass Spectrom. Ion Processes 121 (1992) 111.
[12] T. Walczyk, Int. J. Mass Spectrom. Ion Processes 161 (1997) 217.
[13] W. Compston, V.M. Oversby, J. Geophys. Res. 74 (1969) 4338.
[13] P.D.P. Taylor, R. Maeck, F. Hendrickx, P. De Bièvre, Int. J. Mass Spectrom. Ion Processes 128 (1993) 91.
[14] O. Eugster, F. Tera, G.J. Wasserburg, J. Geophys. Res. 74 (1969) 3897.
[15] N.H. Gale, Chem. Geol. 6 (1970) 305.
[16] G.L. Cumming, Chem. Geol. 11 (1973) 157.
[17] M.J. Dallwitz, Chem. Geol. 6 (1970) 311.
[18] M.H. Dodson, Geochim. Cosmochim. Acta 34 (1970) 1241.
[19] A. Hofmann, Earth Planet. Sci. Lett. 10 (1971) 397.
[20] R.D. Russell, J. Geophys. Res. 76 (1971) 4949.
[21] B. Hamelin, G. Manhes, F. Albarede, C.J. Allègre, Geochim. Cosmochim. Acta 49 (1985) 173.
[22] G. Manhes, J.F. Minster, C.J. Allègre, Earth Planet. Sci. Lett. 39 (1978) 14.
[23] B.L. Beard, C.M. Johnson, L. Cox, H. Sun, K.H. Nealson, C. Aguilar, Science, in press.
[24] B.L. Beard, C.M. Johnson, Geochim. Cosmochim. Acta 63 (1999) 1653.
[25] T.D. Bullen, P.M. McMahon, Mineral Mag. 62A (1998) 255.
[26] G.J. Wasserburg, S.B. Jacobsen, D.J. DePaolo, M.T. McCulloch, T. Wen, Geochim. Cosmochim. Acta 45 (1981) 2311.
[27] S.R. Hart, A. Zindler, Int. J. Mass Spectrom. Ion Processes 89 (1989) 287.
[28] R.N. Clayton, Annu. Rev. Earth Planet. Sci. 21 (1993) 115.
[29] T. Bullen, private communication, 1997.